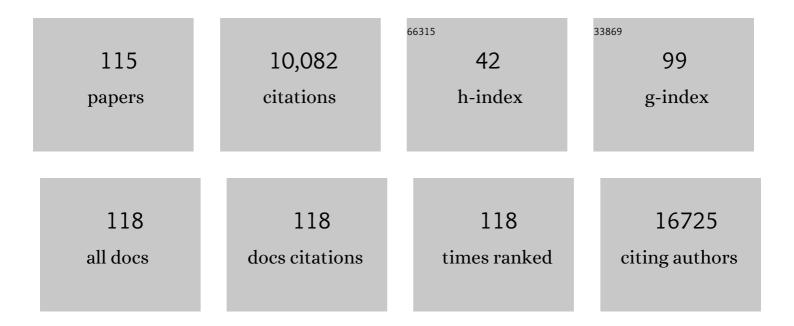
## Chun-Wei Chen

List of Publications by Year in descending order

Source: https://exaly.com/author-pdf/8663159/publications.pdf Version: 2024-02-01



#	Article	IF	CITATIONS
1	Blue Photoluminescence from Chemically Derived Graphene Oxide. Advanced Materials, 2010, 22, 505-509.	11.1	1,824
2	Highly Active and Stable Hybrid Catalyst of Cobalt-Doped FeS <sub>2</sub> Nanosheets–Carbon Nanotubes for Hydrogen Evolution Reaction. Journal of the American Chemical Society, 2015, 137, 1587-1592.	6.6	800
3	Solution-Processable Graphene Oxide as an Efficient Hole Transport Layer in Polymer Solar Cells. ACS Nano, 2010, 4, 3169-3174.	7.3	731
4	Tunable Photoluminescence from Graphene Oxide. Angewandte Chemie - International Edition, 2012, 51, 6662-6666.	7.2	584
5	Advanced rechargeable aluminium ion battery with a high-quality natural graphite cathode. Nature Communications, 2017, 8, 14283.	5.8	453
6	Transparent and conducting electrodes for organic electronics from reduced graphene oxide. Applied Physics Letters, 2008, 92, .	1.5	368
7	Investigation of nanoscale morphological changes in organic photovoltaics during solvent vapor annealing. Journal of Materials Chemistry, 2008, 18, 306-312.	6.7	288
8	Interfacial Nanostructuring on the Performance of Polymer/TiO <sub>2</sub> Nanorod Bulk Heterojunction Solar Cells. Journal of the American Chemical Society, 2009, 131, 3644-3649.	6.6	286
9	Enhancing photoluminescence quenching and photoelectric properties of CdSe quantum dots with hole accepting ligands. Journal of Materials Chemistry, 2008, 18, 675.	6.7	229
10	FeS <sub>2</sub> Nanocrystal Ink as a Catalytic Electrode for Dye‣ensitized Solar Cells. Angewandte Chemie - International Edition, 2013, 52, 6694-6698.	7.2	227
11	A first-principles study of nitrogen- and boron-assisted platinum adsorption on carbon nanotubes. Carbon, 2009, 47, 850-855.	5.4	198
12	Top Laminated Graphene Electrode in a Semitransparent Polymer Solar Cell by Simultaneous Thermal Annealing/Releasing Method. ACS Nano, 2011, 5, 6564-6570.	7.3	188
13	High-Mobility InSe Transistors: The Role of Surface Oxides. ACS Nano, 2017, 11, 7362-7370.	7.3	177
14	Low-Threshold Lasing from 2D Homologous Organic–Inorganic Hybrid Ruddlesden–Popper Perovskite Single Crystals. Nano Letters, 2018, 18, 3221-3228.	4.5	177
15	Cleanâ€Lifting Transfer of Largeâ€area Residualâ€Free Graphene Films. Advanced Materials, 2013, 25, 4521-4526.	11.1	157
16	Intermixing-seeded growth for high-performance planar heterojunction perovskite solar cells assisted by precursor-capped nanoparticles. Energy and Environmental Science, 2016, 9, 1282-1289.	15.6	157
17	Multilayer-graphene-stabilized lithium deposition for anode-Free lithium-metal batteries. Nanoscale, 2019, 11, 2710-2720.	2.8	118
18	The influence of interface modifier on the performance of nanostructured ZnO/polymer hybrid solar cells. Applied Physics Letters, 2009, 94, 063308.	1.5	114

#	Article	IF	CITATIONS
19	Solutionâ€Processable Pyrite FeS <sub>2</sub> Nanocrystals for the Fabrication of Heterojunction Photodiodes with Visible to NIR Photodetection. Advanced Materials, 2012, 24, 3415-3420.	11.1	112
20	Near-ultraviolet photodetector based on hybrid polymer/zinc oxide nanorods by low-temperature solution processes. Applied Physics Letters, 2008, 92, .	1.5	110
21	Extrinsic Origin of Persistent Photoconductivity in Monolayer MoS2 Field Effect Transistors. Scientific Reports, 2015, 5, 11472.	1.6	110
22	Nanostructured metal oxide/conjugated polymer hybrid solar cells by low temperature solution processes. Journal of Materials Chemistry, 2007, 17, 4571.	6.7	103
23	Biologically inspired graphene-chlorophyll phototransistors with high gain. Carbon, 2013, 63, 23-29.	5.4	100
24	Extended red light harvesting in a poly(3-hexylthiophene)/iron disulfide nanocrystal hybrid solar cell. Nanotechnology, 2009, 20, 405207.	1.3	91
25	Grapheneâ€Based Integrated Photovoltaic Energy Harvesting/Storage Device. Small, 2015, 11, 2929-2937.	5.2	90
26	Self-Encapsulated Doping of n-Type Graphene Transistors with Extended Air Stability. ACS Nano, 2012, 6, 6215-6221.	7.3	76
27	Fast growth of large-grain and continuous MoS2 films through a self-capping vapor-liquid-solid method. Nature Communications, 2020, 11, 3682.	5.8	76
28	Substituent Effect on the Optoelectronic Properties of Alternating Fluoreneâ ´´Cyclopentadithiophene Copolymers. Macromolecules, 2008, 41, 6664-6671.	2.2	71
29	Interplay of Three-Dimensional Morphologies and Photocarrier Dynamics of Polymer/TiO2Bulk Heterojunction Solar Cells. Journal of the American Chemical Society, 2011, 133, 11614-11620.	6.6	66
30	Selfâ€Crackâ€Filled Graphene Films by Metallic Nanoparticles for Highâ€Performance Graphene Heterojunction Solar Cells. Advanced Materials, 2015, 27, 1724-1729.	11.1	65
31	Transport/Magnetotransport of High-Performance Graphene Transistors on Organic Molecule-Functionalized Substrates. Nano Letters, 2012, 12, 964-969.	4.5	62
32	Polymer–metal-oxide hybrid solar cells. Journal of Materials Chemistry A, 2013, 1, 10574.	5.2	60
33	Improved charge separation and transport efficiency in poly(3-hexylthiophene)–TiO2 nanorod bulk heterojunction solar cells. Journal of Materials Chemistry, 2008, 18, 2201.	6.7	59
34	Employing an amphiphilic interfacial modifier to enhance the performance of a poly(3-hexyl) Tj ETQq0 0 0 rgBT /	Dverlock 1	0 Tf 50 142 1
35	A Quinone-Based Electrode for High-Performance Rechargeable Aluminum-Ion Batteries with a Low-Cost AlCl <sub>3</sub> /Urea Ionic Liquid Electrolyte. ACS Applied Materials & amp; Interfaces, 2020, 12, 25853-25860	4.0	55

36Atomic-Scale Interfacial Band Mapping across Vertically Phased-Separated Polymer/Fullerene Hybrid4.55336Solar Cells. Nano Letters, 2013, 13, 2387-2392.53

#	Article	IF	CITATIONS
37	Antibacterial property of Ag nanoparticle-impregnated N-doped titania films under visible light. Scientific Reports, 2015, 5, 11978.	1.6	52
38	Spatially Resolved Imaging on Photocarrier Generations and Band Alignments at Perovskite/Pbl <sub>2</sub> Heterointerfaces of Perovskite Solar Cells by Light-Modulated Scanning Tunneling Microscopy. Nano Letters, 2017, 17, 1154-1160.	4.5	50
39	Solution processable nanocarbon platform for polymer solar cells. Energy and Environmental Science, 2011, 4, 3521.	15.6	47
40	Facilely Synthesized spiro[fluoreneâ€9,9′â€phenanthrenâ€10′â€one] in Donor–Acceptor–Donor Holeâ€Transporting Materials for Perovskite Solar Cells. ChemSusChem, 2018, 11, 3225-3233.	3.6	47
41	Selfâ€Assembly Atomic Stacking Transport Layer of 2D Layered Titania for Perovskite Solar Cells with Extended UV Stability. Advanced Energy Materials, 2018, 8, 1701722.	10.2	46
42	Regioregularity effects in the chain orientation and optical anisotropy of composite polymer/fullerene films for high-efficiency, large-area organic solar cells. Journal of Materials Chemistry, 2009, 19, 5554.	6.7	44
43	Surface Oxidation Doping to Enhance Photogenerated Carrier Separation Efficiency for Ultrahigh Gain Indium Selenide Photodetector. ACS Photonics, 2017, 4, 2930-2936.	3.2	44
44	Growth and characterization of nonpolar ZnO () epitaxial film on Î <sup>3</sup> -LiAlO2 substrate by chemical vapor deposition. Journal of Crystal Growth, 2007, 308, 412-416.	0.7	42
45	Sunlight-activated graphene-heterostructure transparent cathodes: enabling high-performance n-graphene/p-Si Schottky junction photovoltaics. Energy and Environmental Science, 2015, 8, 2085-2092.	15.6	42
46	Intrinsic Carrier Transport of Phaseâ€Pure Homologous 2D Organolead Halide Hybrid Perovskite Single Crystals. Small, 2018, 14, e1803763.	5.2	42
47	Electric field-assisted self-organization of polymer:fullerene hybrids on the photovoltaic performance. Energy and Environmental Science, 2011, 4, 2134.	15.6	41
48	Polarization-dependent confocal Raman microscopy of an individual ZnO nanorod. Applied Physics Letters, 2008, 92, .	1.5	40
49	Enhanced Charge Separation by Sieve‣ayer Mediation in Highâ€Efficiency Inorganicâ€Organic Solar Cells. Advanced Materials, 2009, 21, 759-763.	11.1	39
50	Precisely Controlled Ultrastrong Photoinduced Doping at Graphene–Heterostructures Assisted by Trap‧tateâ€Mediated Charge Transfer. Advanced Materials, 2015, 27, 7809-7815.	11.1	39
51	Quantitative nanoscale monitoring the effect of annealing process on the morphology and optical properties of poly(3-hexylthiophene)/[6,6]-phenyl C61-butyric acid methyl ester thin film used in photovoltaic devices. Journal of Applied Physics, 2009, 106, 034506.	1.1	38
52	Photodriven Dipole Reordering: Key to Carrier Separation in Metalorganic Halide Perovskites. ACS Nano, 2019, 13, 4402-4409.	7.3	38
53	Nanoscale morphology and performance of molecular-weight-dependent poly(3-hexylthiophene)/TiO2 nanorod hybrid solar cells. Journal of Materials Chemistry, 2008, 18, 4097.	6.7	36
54	High-Performance InSe Transistors with Ohmic Contact Enabled by Nonrectifying Barrier-Type Indium Electrodes. ACS Applied Materials & Interfaces, 2018, 10, 33450-33456.	4.0	35

#	Article	IF	CITATIONS
55	Quantum Dot Light-Emitting Diode Using Solution-Processable Graphene Oxide as the Anode Interfacial Layer. Journal of Physical Chemistry C, 2012, 116, 10181-10185.	1.5	31
56	Unravelling the origin of the photocarrier dynamics of fullerene-derivative passivation of SnO <sub>2</sub> electron transporters in perovskite solar cells. Journal of Materials Chemistry A, 2020, 8, 23607-23616.	5.2	30
57	Layer-by-layer thin film of reduced graphene oxide and gold nanoparticles as an effective sample plate in laser-induced desorption/ionization mass spectrometry. Analytica Chimica Acta, 2014, 809, 97-103.	2.6	28
58	Iron Pyrite/Titanium Dioxide Photoanode for Extended Near Infrared Light Harvesting in a Photoelectrochemical Cell. Scientific Reports, 2016, 6, 20397.	1.6	27
59	Unveiling the Nanoparticleâ€Seeded Catalytic Nucleation Kinetics of Perovskite Solar Cells by Timeâ€Resolved GIXS. Advanced Functional Materials, 2019, 29, 1902582.	7.8	27
60	Atomic-Layer Controlled Interfacial Band Engineering at Two-Dimensional Layered PtSe <sub>2</sub> /Si Heterojunctions for Efficient Photoelectrochemical Hydrogen Production. ACS Nano, 2021, 15, 4627-4635.	7.3	27
61	Enhancement of laser action in ZnO nanorods assisted by surface plasmon resonance of reduced graphene oxide nanoflakes. Optics Express, 2012, 20, A799.	1.7	26
62	Wavelengthâ€Selective Dual p―and nâ€Type Carrier Transport of an Organic/Graphene/Inorganic Heterostructure. Advanced Materials, 2015, 27, 282-287.	11.1	26
63	Photoluminescence quenching of graphene oxide by metal ions in aqueous media. Carbon, 2015, 82, 24-30.	5.4	26
64	Nanoscale Morphology Control of Polymer/TiO <sub>2</sub> Nanocrystal Hybrids: Photophysics, Charge Generation, Charge Transport, and Photovoltaic Properties. Journal of Physical Chemistry C, 2010, 114, 18717-18724.	1.5	25
65	Gas molecule effects on field emission properties of single-walled carbon nanotube. Diamond and Related Materials, 2004, 13, 1306-1313.	1.8	24
66	Polymer/Metal Oxide Nanocrystals Hybrid Solar Cells. IEEE Journal of Selected Topics in Quantum Electronics, 2010, 16, 1635-1640.	1.9	24
67	Exploring the Origin of Phase-Transformation Kinetics of CsPbI <sub>3</sub> Perovskite Nanocrystals Based on Activation Energy Measurements. Journal of Physical Chemistry Letters, 2020, 11, 3287-3293.	2.1	23
68	Metallic Nanowire Coupled CsPbBr <sub>3</sub> Quantum Dots Plasmonic Nanolaser. Advanced Functional Materials, 2021, 31, 2102375.	7.8	23
69	Creation of 3D Textured Graphene/Si Schottky Junction Photocathode for Enhanced Photoâ€Electrochemical Efficiency and Stability. Advanced Energy Materials, 2019, 9, 1901022.	10.2	21
70	Enhanced infrared light harvesting of inorganic nanocrystal photovoltaic and photodetector on graphene electrode. Applied Physics Letters, 2011, 98, 263509.	1.5	20
71	Tunable Photoinduced Carrier Transport of a Black Phosphorus Transistor with Extended Stability Using a Light-Sensitized Encapsulated Layer. ACS Photonics, 2016, 3, 1102-1108.	3.2	20
72	Critical Intermediate Structure That Directs the Crystalline Texture and Surface Morphology of Organo-Lead Trihalide Perovskite. ACS Applied Materials & Interfaces, 2017, 9, 36897-36906.	4.0	20

#	Article	IF	CITATIONS
73	Oxidized-monolayer tunneling barrier for strong Fermi-level depinning in layered InSe transistors. Npj 2D Materials and Applications, 2019, 3, .	3.9	19
74	Twoâ€Ðimensional Bis(dithiolene)iron(II) Selfâ€Powered UV Photodetectors with Ultrahigh Air Stability. Advanced Science, 2021, 8, 2100564.	5.6	19
75	Influence of Solvent on the Dispersion of Single-Walled Carbon Nanotubes in Polymer Matrix and the Photovoltaic Performance. Journal of Physical Chemistry C, 2010, 114, 10932-10936.	1.5	16
76	Correlation of nanoscale organizations of polymer and nanocrystals in polymer/inorganic nanocrystal bulk heterojunction hybrid solar cells: insights from multiscale molecular simulations. Energy and Environmental Science, 2013, 6, 307-315.	15.6	16
77	Bulk intermixing-type perovskite CH <sub>3</sub> NH <sub>3</sub> PbI <sub>3</sub> /TiO <sub>2</sub> nanorod hybrid solar cells. Nanoscale, 2015, 7, 14532-14537.	2.8	15
78	Effects of surface oxidation of Cu substrates on the growth kinetics of graphene by chemical vapor deposition. Nanoscale, 2017, 9, 2324-2329.	2.8	14
79	Visualizing band alignment across 2D/3D perovskite heterointerfaces of solar cells with light-modulated scanning tunneling microscopy. Nano Energy, 2021, 89, 106362.	8.2	13
80	Quantum-assisted photoelectric gain effects in perovskite solar cells. NPG Asia Materials, 2020, 12, .	3.8	12
81	Residue-free fabrication of high-performance graphene devices by patterned PMMA stencil mask. AIP Advances, 2014, 4, .	0.6	11
82	Stoichiometric dependence of TiOx as a cathode modifier on band alignment of polymer solar cells. Solar Energy Materials and Solar Cells, 2014, 125, 233-238.	3.0	11
83	Wavelength-dependent optical transition mechanisms for light-harvesting of perovskite MAPbI3 solar cells using first-principles calculations. Journal of Materials Chemistry C, 2016, 4, 5248-5254.	2.7	11
84	Environment-insensitive and gate-controllable photocurrent enabled by bandgap engineering of MoS2 junctions. Scientific Reports, 2017, 7, 44768.	1.6	11
85	Origin of Extended UV Stability of 2D Atomic Layer Titania-Based Perovskite Solar Cells Unveiled by Ultrafast Spectroscopy. ACS Applied Materials & Interfaces, 2019, 11, 21473-21480.	4.0	11
86	Strong Excitonic Magneto-Optic Effects in Two-Dimensional Organic–Inorganic Hybrid Perovskites. ACS Applied Materials & Interfaces, 2021, 13, 10279-10286.	4.0	11
87	Segmented Highly Reversible Thermochromic Layered Perovskite [(CH <sub>2</sub> ) <sub>2</sub> (NH <sub>3</sub> ) <sub>2</sub> ]CuCl <sub>4</sub> Crystal Coupled with an Inverse Magnetocaloric Effect. ACS Applied Electronic Materials, 2022, 4, 521-530.	2.0	11
88	Dependence of Nanocrystal Dimensionality on the Polymer Nanomorphology, Anisotropic Optical Absorption, and Carrier Transport in P3HT:TiO <sub>2</sub> Bulk Heterojunctions. Journal of Physical Chemistry C, 2012, 116, 25081-25088.	1.5	10
89	Clean water generation through a multifunctional activated carbon-TiO <sub>2</sub> interfacial solar distillation system. RSC Advances, 2021, 11, 23036-23044.	1.7	10
90	Using Exciton/Trion Dynamics to Spatially Monitor the Catalytic Activities of MoS <sub>2</sub> during the Hydrogen Evolution Reaction. ACS Nano, 2022, 16, 4298-4307.	7.3	10

#	Article	IF	CITATIONS
91	Integration of on-chip perovskite nanocrystal laser and long-range surface plasmon polariton waveguide with etching-free process. Nanoscale, 2022, 14, 10075-10081.	2.8	9
92	Atomically Resolved Quantum-Confined Electronic Structures at Organic–Inorganic Interfaces of Two-Dimensional Ruddlesden–Popper Halide Perovskites. Nano Letters, 2021, 21, 8066-8072.	4.5	8
93	Growth behavior and microstructure of ZnO epilayer on γâ€LiAlO <sub>2</sub> (100) substrate by chemical vapor deposition. Physica Status Solidi (A) Applications and Materials Science, 2009, 206, 215-219.	0.8	7
94	Interactions between fluorescence of atomically layered graphene oxide and metallic nanoparticles. Nanoscale, 2013, 5, 1687.	2.8	7
95	Stabilized Highâ€Membered and Phaseâ€Pure 2D All Inorganic Ruddlesden–Popper Halide Perovskites Nanocrystals as Photocatalysts for the CO <sub>2</sub> Reduction Reaction. Small, 2022, 18, e2107881.	5.2	7
96	Studies of Electronic Excitations of Rectangular ZnO Nanorods by Electron Energy-Loss Spectroscopy. Plasmonics, 2012, 7, 123-130.	1.8	6
97	Lithographic in-mold patterning for CsPbBr <sub>3</sub> nanocrystals distributed Bragg reflector single-mode laser. Nanoscale, 2021, 13, 15830-15836.	2.8	6
98	Direct investigation of the reorientational dynamics of A-site cations in 2D organic-inorganic hybrid perovskite by solid-state NMR. Nature Communications, 2022, 13, 1513.	5.8	6
99	Observation of quantum Hall plateau-plateau transition and scaling behavior of the zeroth Landau level in graphene <mml:math xmlns:mml="http://www.w3.org/1998/Math/MathML"&gt;<mml:mrow><mml:mi>p</mml:mi><mml:mtext>â^'Physical Review B. 2016. 93</mml:mtext></mml:mrow></mml:math 	:mtext> <r< td=""><td>nml:mi&gt;n</td></r<>	nml:mi>n
100	Selfâ€Patterned CsPbBr <sub>3</sub> Nanocrystal Based Plasmonic Hotâ€Carrier Photodetector at Telecommunications Wavelengths. Advanced Optical Materials, 2021, 9, 2101474.	3.6	5
101	Phase Modulation of Self-Gating in Ionic Liquid-Functionalized InSe Field-Effect Transistors. Nano Letters, 2022, 22, 2270-2276.	4.5	5
102	Anisotropic surface plasmon excitation in Au/silica nanowire. Applied Physics Letters, 2010, 96, 263106.	1.5	4
103	Water Splitting: Creation of 3D Textured Graphene/Si Schottky Junction Photocathode for Enhanced Photoâ€Electrochemical Efficiency and Stability (Adv. Energy Mater. 29/2019). Advanced Energy Materials, 2019, 9, 1970115.	10.2	4
104	Magnetic Dipole Resonance and Coupling Effects Directly Enhance the Raman Signals of As-Grown Graphene on Copper Foil by over One Hundredfold. Chemistry of Materials, 2018, 30, 1472-1483.	3.2	3
105	Internal Built-In Electric Fields at Organic–Inorganic Interfaces of Two-Dimensional Ruddlesden–Popper Perovskite Single Crystals. ACS Applied Materials & Interfaces, 2022, 14, 19818-19825.	4.0	3
106	Dual Functional Polymer Interlayer for Facilitating Ion Transport and Reducing Charge Recombination in Dye-Sensitized Solar Cells. ACS Applied Materials & Interfaces, 2016, 8, 33666-33672.	4.0	2
107	Spatially and Precisely Controlled Large-Scale and Persistent Optical Gating in a TiOx–MoS2 Heterostructure. ACS Applied Materials & Interfaces, 2018, 10, 38319-38325.	4.0	2
108	Self-assembly nuclei with a preferred orientation at the extended hydrophobic surface toward textured growth of ZnO nanorods in aqueous chemical bath deposition. Nanotechnology, 2021, 32, 175603.	1.3	2

#	Article	IF	CITATIONS
109	Growth and Optical Properties of Nonpolar (\$10{ar {1}}0\$) Zn <sub>1â€<i>x</i></sub> Co <sub><i>x</i></sub> O Epitaxial Film on a <i>γ</i> â€LiAlO <sub>2</sub> Substrate. Chemical Vapor Deposition, 2011, 17, 88-92.	1.4	1
110	Superconductivity observed in platinum-silicon interface. Applied Physics Letters, 2014, 104, 211604.	1.5	1
111	Interlayer Interaction Induced Layer-Dependent Catalytic Activity toward a Hydrogen Evolution Reaction on Two-Dimensional PtSe2. Journal of Physical Chemistry C, 2021, 125, 19716-19723.	1.5	1
112	Selfâ€Patterned CsPbBr <sub>3</sub> Nanocrystal Based Plasmonic Hotâ€Carrier Photodetector at Telecommunications Wavelengths (Advanced Optical Materials 24/2021). Advanced Optical Materials, 2021, 9, .	3.6	1
113	Work function evolution of graphene oxide by utilizing hydrothermal treatment. , 2010, , .		0
114	Photovoltaic and optoelectronic applications of large-area graphene-based electronics. , 2010, , .		0
115	Solid-State NMR Characterization of the Reorientational Dynamics of A-site Cations in 2D OIHPs. , 0, , .		0